

# Supplementary File for “A New Knowledge Mining and Root Cause Analysis Methodology for Multivariate Time Series”

THIS part provides the supplementary material to support the research in the paper.

## I. PRELIMINARIES

Notations adopted in this paper are summarized in Table S-I.

## II. MODELING WITH SBTPN

The SBTPN defined in Section IV of the paper has two key characteristics: the integration of Petri net (PN) transitions into the probability distribution of Bayesian networks (BNs), and the introduction of synergy effects into BNs.

The necessity of the first key characteristic of SBTPN, namely the integration of PN transitions into the probability distribution of BNs, is discussed first. Given that BNs can perform interpretable probabilistic reasoning under uncertainty, they are employed as the fundamental architecture for the proposed RCA method. However, BNs do not explicitly emphasize “AND/OR” relations, which increases the complexity of constructing BNs. Consider the following two chemical reactions: 1) Reaction  $a$ :  $A \rightarrow D$ , where  $A$  and  $D$  are the reactant and product of  $a$ , respectively; and 2) Reaction  $b$ :  $B + C \rightarrow D$ , where  $B$  and  $C$  are the reactants of  $b$ , and  $D$  is its product. The causal relations among  $A$ ,  $B$ ,  $C$ , and  $D$  can be expressed by the following causal rules:  $R_1$ : IF “Reactant  $A$  exists” THEN “Product  $D$  appears” and  $R_2$ : IF “Reactant  $B$  exists” AND “Reactant  $C$  exists” THEN “Product  $D$  appears”. Fig. S1(a) illustrates the idea of modeling the above reactions using a BN. Note that, throughout this paper,  $\hat{x}$  or  $\check{x}$  denotes the state of a variable, place or transition corresponding to  $x$ . For a variable or place, its state is “true” or “false”. As to a transition, its state is “enabled” or “disabled”. From Fig. S1(a), the BN fails to directly depict the “AND” relation between variables  $B$  and  $C$ . This leads to high complexity in constructing the conditional probability table (CPT)  $M_1$ .

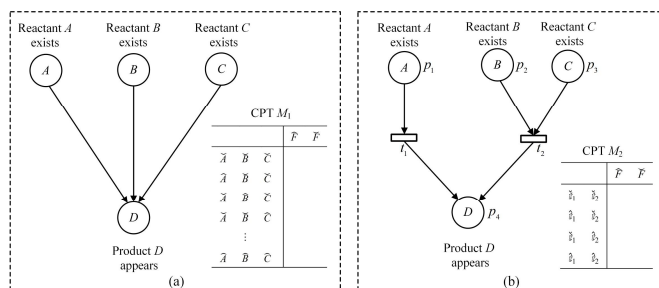


Fig. S1. Difference between a BN and the modeling paradigm to be proposed. (a) BN model instance and (b) Modeling paradigm to be proposed.

As shown in Fig. S1(b), the complexity of constructing a CPT can be reduced by integrating the causal variables within the same “AND” structure into a single one. In Fig. S1(b), a

PN place (represented by a circle) is used to depict a causal or effect variable. A PN transition (represented by a rectangle) is used to model a causal rule. The causal variable is expressed as the input place of a transition. Causal variables that point to the same transition have an “AND” relation. The effect variable is expressed as the output place of a transition. A solid arc represents the flow relation from a causal variable to a transition (or from a transition to an effect variable). As shown in Fig. S1(b), transitions  $t_1$  and  $t_2$  are used to model rule  $R_1$ : IF “Reactant  $A$  exists” THEN “Product  $D$  appears” and rule  $R_2$ : IF “Reactant  $B$  exists” AND “Reactant  $C$  exists” THEN “Product  $D$  appears”, respectively. The probability that proposition “Product  $D$  appears” holds depends on the probability that either  $R_1$  or  $R_2$  is activated. Therefore, CPT  $M_2$  can be determined by identifying whether  $R_1$  or  $R_2$  is activated. Clearly, the complexity of constructing  $M_2$  is lower than that of constructing  $M_1$ .

From the perspective of knowledge representation, the “AND” relation can be represented by integrating all cause variables within the same “AND” structure into an additional BN variable. However, from the perspective of knowledge mining, causal discovery methods aim to discover the causal relations among observed variables. Because the additional variable does not exist in the original data, it is impossible to directly discover the causal relation between it and other variables in the BN from the data. Modeling “AND” relations with PN transitions does not suffer from this limitation, because they are only used to constrain the causal relations among observed variables. By associating all cause variables in an “AND” structure with a PN transition, and incorporating the transition as an additional node into BN, the complexity of constructing the CPT for BN can be reduced. This approach also enables BN to depict “AND/OR” relations and synergy effects during RCA.

The importance of the second key characteristic of SBTPN, namely the introduction of synergy effects into BNs, is discussed next. Causal models, including BNs and PN, fail to depict synergy effects. They treat a synergy factor as either a causal or non-causal variable of the effect one, which can affect the reliability of causality-driven RCA. Consider the chemical reaction  $a$ :  $A \xrightarrow{B} C$ , where  $A$  is the reactant, and  $B$  and  $C$  are the inhibitor (a substance that slows down a chemical reaction or prevents it from occurring) and product, respectively. Essentially,  $A$  is the cause of the production of  $C$ , but  $B$  is not its cause. However,  $B$  can affect the production of  $C$ . Specifically, reaction  $a$  is harder to carry out under the action of inhibitor  $B$ , i.e.,  $B$  has an inhibitory effect on  $a$ . In a rule-based system, such phenomena can be expressed as: A non-causal variable can affect the probability that a reasoning

TABLE S-I  
NOTATIONS

Symbol	Description
$X$	Set of variables.
$P$	Set of places.
$T$	Set of transitions.
${}^\circ t$	Set of places that have synergy effects on transition $t$ .
$p^\circ$	Set of transitions affected by the synergy effects of place $p$ .
$\beta(p)$	Variable associated with place $p$ .
$\text{Pr}(\cdot)$	Probability function.
$\cdot v / v \cdot$	Pre-set/post-set of a node $v \in P \cup T$ .
$\hat{p} / \check{p}$	State of place $p$ , indicating that $\beta(p)$ is present/absent.
$\hat{t} / \check{t}$	State of transition $t$ , indicating that $t$ is enabled/disabled.
$a_{ij}$	Attention score that is used to determine whether $x_i$ is the cause of $x_j$ .
$w_{ij}$	Kernel weight that is used to calculate the time delay of the impact of $x_i$ on $x_j$ .
$e_{ij}$	Time delay of the impact of $x_i$ on $x_j$ .
$\zeta$	Total number of time steps of a time series.
$\mu_{ij}^\tau$	Impact of $x_i$ on $x_j$ at time step $\tau$ .
$\Phi(x_i, x_j, x_k)$	Strength of the ‘‘AND’’ relation between $x_i$ and $x_j$ pointing to $x_k$ .
$\mathbb{N}_h$	$\{1, 2, \dots, h\}$ .
$\Psi(t_k; t'_k; p_x) / \Upsilon(t_k; t'_k; p_x)$	Strength of the catalytic/inhibitory effect of $p_x$ on $t_k$ .
$\eta_1 / \eta_2$	Threshold for determining a catalytic/ inhibitory effect.
$\mathbb{C}(t_k) / \mathbb{I}(t_k)$	Set of places that have catalytic/inhibitory effects on $t_k$ .

rule holds. In this paper, if a non-causal variable can reduce (increase) the probability that a reasoning rule holds, the variable is said to have an inhibitory (catalytic) effect on the rule.

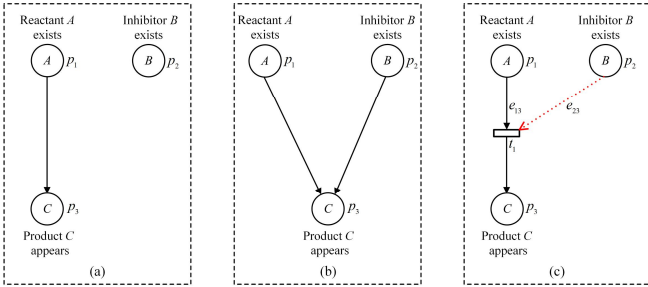


Fig. S2. Knowledge modeling for the chemical reaction. (a) and (b) BN modelling paradigms, and (c) proposed modelling paradigm.

Figs. S2(a) and (b) show the results of modeling the aforementioned reaction based on BNs. Next, the reason for the existence of  $C$  is discussed based on the causal structures shown in Figs. S2(a) and (b). Consider the case where reactant  $A$ , inhibitor  $B$ , and product  $C$  are present. From Fig. S2(a), reactant  $A$  is the reason for the presence of product  $C$  in this case. It can be inferred from Fig. S2(b) that in this case, both reactant  $A$  and inhibitor  $B$  are the reasons for the existence of product  $C$ . In fact, inhibitor  $B$  can block the causal relation between reactant  $A$  and product  $C$ . Therefore, in this case, neither reactant  $A$  nor inhibitor  $B$  is the reason for the presence of product  $C$ . From Figs. S2(a) and (b), traditional BNs fail to depict synergy effects, thus affecting the credibility of RCA. To characterize the impact of synergy effects on RCA, this

paper uses PNs to model the synergy effects constrained by time. Specifically, a synergy relation is defined from a place to a transition to depict the synergy effects of non-causal variables on causal rules. The weight assigned to the synergy relation indicates the time delay in the generation of the synergy effect. A red dotted (green dashed) arc represents an inhibitory (catalytic) effect. Fig. S2(c) shows the proposed modelling paradigm, which can accurately model the synergy effects constrained by time.

### III. SBTPN STRUCTURE MINING

Fig. S3 shows the proposed methodology. Its basic idea is as follows: 1) learning simple temporal causal relations from MTS; 2) mining the ‘‘AND/OR’’ relations constrained by time based on the discovered causal relations; 3) discovering the synergy effects constrained by time based on the identified ‘‘AND/OR’’ relations; and 4) implementing RCA based on the ‘‘AND/OR’’ relations and synergy effects.

#### A. Learning Simple Temporal Causal Relations

This study leverages the temporal causal discovery framework (TCDF) proposed in [1] to learn simple temporal causal relations. It is a 1D dilated convolutional neural network and its structure is called Attention-based Dilated Depthwise Separable Temporal Convolutional Network (AD-DSTCN). As shown in Fig. S3, each time series  $x_j$ ,  $j \in \{1, 2, \dots, m\}$  is associated with an AD-DSTCN  $j$  that is composed of  $m$  dilated convolutional neural networks (DCNNs) with 1D kernels. The input of DCNN  $i \in \{1, 2, \dots, m\}$

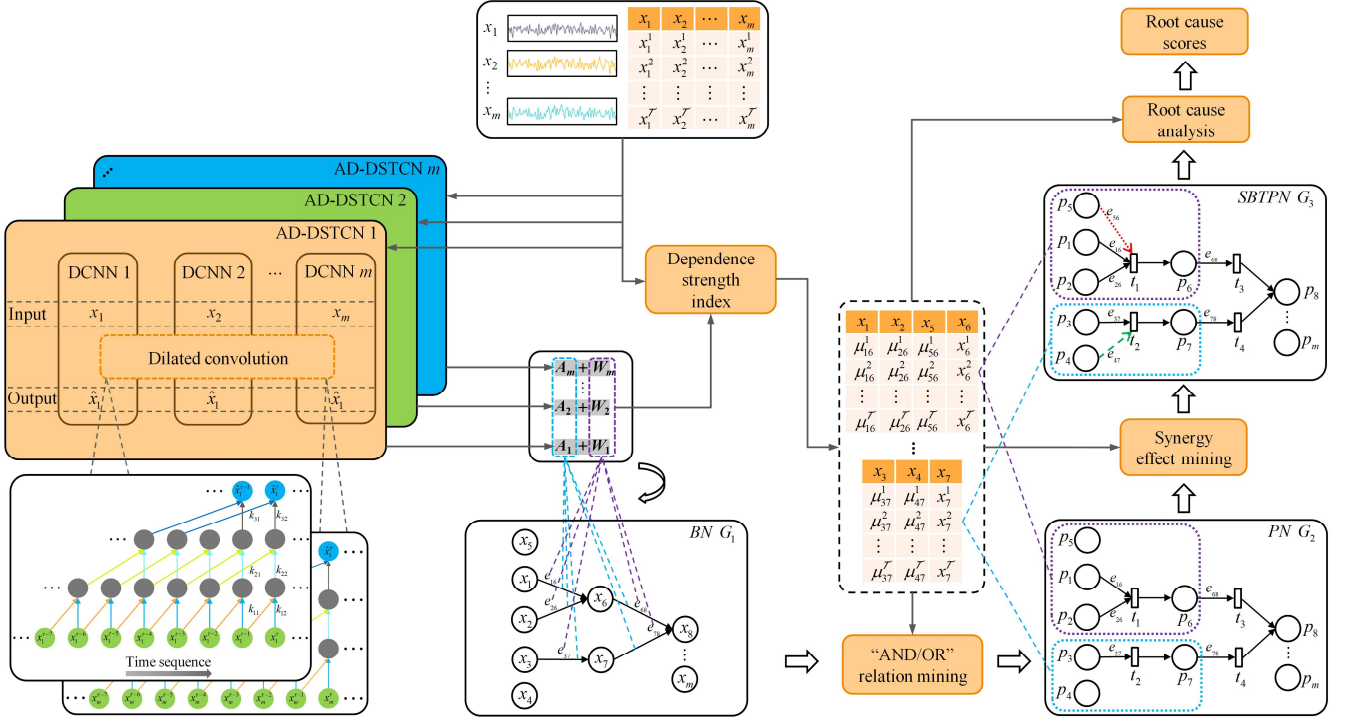


Fig. S3. Schematic diagram of the proposed methodology.

in AD-DSTCN  $j$  is a time series  $x_i$  and its outputs are the predictive value  $\hat{x}_j$ , the attention score  $a_{ij}$  that is used to determine whether  $x_i$  is the cause of  $x_j$ , and the kernel weight  $w_{ij}$  that is used to calculate the time delay of the impact of  $x_i$  on  $x_j$ . Vectors  $A_j = [a_{1j}, a_{2j}, \dots, a_{mj}]$  and  $W_j = [w_{1j}, w_{2j}, \dots, w_{mj}]$  are used to determine the causes of  $x_j$  and the time delays of causal effects between  $x_j$  and its causes, respectively. As seen in Fig. S3, TCDF outputs a simple temporal causal graph  $G_1$ .

The idea for discovering simple temporal causal relations is discussed in Algorithm 1.

**Algorithm 1** Discovering simple temporal causal relation

**Input:** A dataset  $\partial$  composed of MTS  $X = \{x_1, x_2, \dots, x_m\}$ .

**Output:** A simple temporal causal graph  $G_1$ .

- 1: Build a TCDF consisting of  $m$  AD-DSTCNs for  $X$ ;
- 2: **for**  $j = 1, 2, \dots, m$  **do**
- 3: Construct AD-DSTCN  $j$  whose input is  $\partial$  and goal is to predict  $x_j$ ;
- 4: Generate an attention score vector  $A_j$  and a kernel weight vector  $W_j$  using AD-DSTCN  $j$ ;
- 5: Using  $A_j$  to identify the direct causes of  $x_j$ ;
- 6: Using  $W_j$  to determine the time delays of  $x_j$ 's direct causes affecting  $x_j$ ;
- 7: **end for**
- 8: **return** a simple temporal causal graph  $G_1$

**B. Mining "AND/OR" Relations Constrained by Time**

This study leverages the causal graph  $G_1$  in Fig. S3 learned by TCDF to mine the "AND/OR" relations constrained by time.

Let  $Parents(G_1, x_k)$  denote the set of causes of time series  $x_k$  in  $G_1$ . Given two time series  $x_i, x_j \in Parents(G_1, x_k)$ , the function  $\Phi(x_i, x_j, x_k)$  in (4) in the paper is used to determine whether there is an "AND" relation between  $x_i$  and  $x_j$  pointing to  $x_k$ . This work supposes that this "AND" relation exists only if  $\Phi(x_i, x_j, x_k) > 0.5$  and  $\Phi(x_j, x_i, x_k) > 0.5$ . For  $\forall Q_i \subset Parents(G_1, x_k)$  such that  $\forall x_i, x_j \in Q_i : \Phi(x_i, x_j, x_k) > 0.5 \wedge \Phi(x_j, x_i, x_k) > 0.5$ ,  $Q_i$  is added to a set denoted by  $AND(G_1, x_k)$ , which depicts all the "AND" relations among the causes of  $x_k$ . For  $\forall x_i \in Parents(G_1, x_k) - AND(G_1, x_k)$ , it is added to a set denoted by  $T_{associ}(G_1, x_k)$  along with  $Q_i$ , which depicts all the "AND/OR" relations among the causes of  $x_k$ .  $T_{associ}(G_1, x_k)$  can be mapped to a place set  $T_{associ}(G_1, p_k) = \{p_i, Q_i^*\}$  such that  $\beta(p_k) = x_k$ ,  $\beta(p_i) = x_i$ , and  $\forall p_j \in Q_i^* \exists x_j \in Q_i : \beta(p_j) = x_j$ . Each  $Q_i^*$  (or  $p_i$ ) in  $T_{associ}(G_1, p_k)$  is associated with a transition  $t_j$  satisfying  $t_j = Q_i^*$  (or  $t_j = p_i$ ) and  $t_j^* = p_k$ . For  $\forall p_i \in t_j$ , the directed arcs from  $p_i$  to  $t_j$  and from  $t_j$  to  $p_k$  are defined. The weight  $e_{ik}$  on the arc from  $p_i$  to  $t_j$  represents the time delay of variable  $\beta(p_i)$  affecting variable  $\beta(p_k)$ , which can be calculated by Definition 2 in the paper. Then, PN  $G_2$  in Fig.

S3, which considers the “AND/OR” relations constrained by time, can be obtained.

*Example 1:* For the variables  $x_1, x_2, x_3, x_6, x_7,$  and  $x_8$  in the causal graph  $G_1$  in Fig. S3, we have  $Parents(G_1, x_1) = \emptyset$ ,  $Parents(G_1, x_2) = \emptyset$ ,  $Parents(G_1, x_3) = \emptyset$ ,  $Parents(G_1, x_6) = \{\{x_1\}, \{x_2\}\}$ ,  $Parents(G_1, x_7) = \{\{x_3\}\}$ , and  $Parents(G_1, x_8) = \{\{x_6\}, \{x_7\}\}$ . Suppose  $\Phi(x_1, x_2, x_6) > 0.5$ ,  $\Phi(x_2, x_1, x_6) > 0.5$ ,  $\Phi(x_6, x_7, x_8) < 0.5$ , and  $\Phi(x_7, x_6, x_8) < 0.5$ , we have  $AND(G_1, x_1) = \emptyset$ ,  $AND(G_1, x_2) = \emptyset$ ,  $AND(G_1, x_3) = \emptyset$ ,  $AND(G_1, x_6) = \{\{x_1, x_2\}\}$ ,  $AND(G_1, x_7) = \emptyset$ , and  $AND(G_1, x_8) = \emptyset$ . Then, we can get  $T_{associ}(G_1, x_1) = \emptyset$ ,  $T_{associ}(G_1, x_2) = \emptyset$ ,  $T_{associ}(G_1, x_3) = \emptyset$ ,  $T_{associ}(G_1, x_6) = \{\{x_1, x_2\}\}$ ,  $T_{associ}(G_1, x_7) = \{\{x_3\}\}$ , and  $T_{associ}(G_1, x_8) = \{\{x_6\}, \{x_7\}\}$ . These “AND/OR” relations can be depicted by PN  $G_2$  in Fig. S3, where  $t_1 = \{p_1, p_2\}$ ,  $t_2 = \{p_6\}$ ,  $t_3 = \{p_3\}$ ,  $t_4 = \{p_7\}$ ,  $t_5 = \{p_6\}$ ,  $t_6 = \{p_8\}$ ,  $t_7 = \{p_7\}$ , and  $t_8 = \{p_8\}$ . The time delays corresponding to these “AND/OR” relations, which can be derived by using Definition 2, are expressed as  $E(p_1, p_6) = e_{16}$ ,  $E(p_2, p_6) = e_{26}$ ,  $E(p_3, p_7) = e_{37}$ ,  $E(p_6, p_8) = e_{68}$ , and  $E(p_7, p_8) = e_{78}$ .

The idea for mining the “AND/OR” relations constrained by time is realized via Algorithm 2.

---

**Algorithm 2** Mining “AND” relations constrained by time

**Input:** MTS  $X$  with dataset  $\partial$ ; causal graph  $G_1$  learned by Algorithm 1.

**Output:** A PN-based temporal causal graph  $G_2$ .

```

1: for  $\forall x_k \in X$  do
2:   for  $\forall Q_i \subset Parents(G_1, x_k)$  do
3:     if  $\forall x_i, x_j \in Q_i: \Phi(x_i, x_j, x_k) > 0.5 \wedge \Phi(x_j, x_i, x_k) > 0.5$  then
4:       Add  $Q_i$  to  $AND(G_1, x_k)$ ;
5:     end if
6:   end for
7:   for  $\forall Q_i, Q_j \subset AND(G_1, x_k) \wedge Q_i \subset Q_j$  do
8:     Remove  $Q_i$  from  $AND(G_1, x_k)$ ;
9:   end for
10:  Add  $AND(G_1, x_k)$  to  $T_{associ}(G_1, x_k)$ ;
11:  for  $\forall x_l \in Parents(G_1, x_k) - AND(G_1, x_k)$  do
12:    Add  $x_l$  to  $T_{associ}(G_1, x_k)$ ;
13:  end for
14:  Map  $T_{associ}(G_1, x_k)$  to  $T_{associ}(G_1, p_k)$ ;
15:  for  $\forall p_i \in T_{associ}(G_1, p_k)$  do
16:    Let  $E(p_i, p_k) = e_{ik}$ , where  $e_{ik}$  is calculated by Definition 2;
17:  end for
18: end for
19: return a PN-based temporal causal graph  $G_2$ 

```

---

C. Discovering Synergy Effects Constrained by Time

Based on PN  $G_2$  in Fig. S3, this section proposes a method

for mining the synergy effects constrained by time.

Neglecting the direction of the directed edges in  $G_2$  yields an undirected graph. For transition  $t_k$  in the undirected graph, let  $RelatedPlaces(t_k)$  be the set of all the places located in the same connected component as  $t_k$ , and  $UnrelatedPlaces(t_k) = P - RelatedPlaces(t_k)$  be the set of the places that may have synergy effects on  $t_k$ . Given place  $p_x \in UnrelatedPlaces(t_k)$ , the function  $\Psi(\cdot; t_k; t_k'; p_x)$  ( $\Upsilon(\cdot; t_k; t_k'; p_x)$ ) in (5) in the paper is used to determine whether  $p_x$  has a catalytic (inhibitory) effect on  $t_k$ . Let  $\eta_1$  and  $\eta_2$  denote the thresholds for determining a catalytic effect and an inhibitory one, respectively, which satisfy  $\eta_1, \eta_2 \in [0.5, 1)$ . If  $\Psi(\cdot; t_k; t_k'; p_x) > \eta_1$ ,  $p_x$  has a catalytic effect on  $t_k$  and a green dashed arc from  $p_x$  to  $t_k$  is defined. If  $\Upsilon(\cdot; t_k; t_k'; p_x) > \eta_2$ ,  $p_x$  has an inhibitory effect on  $t_k$  and a red dotted arc from  $p_x$  to  $t_k$  is defined. We set  $\eta_1 = 0.51$  and  $\eta_2 = 0.54$ . Given  $p_j = t_k'$ , the weight  $e_{xj}$  on the dashed/dotted arc from  $p_x$  to  $t_k$  indicates the time delay of variable  $\beta(p_x)$  affecting variable  $\beta(p_j)$ , which can be calculated by Definition 2 in the paper. Then, SBTPN  $G_3$  in Fig. S3, which considers the “AND/OR” relations and synergy effects constrained by time, can be derived.

*Example 2:* For the transitions  $t_1$  and  $t_2$  in PN  $G_2$  in Fig. S3, we have  $RelatedPlaces(t_1) = RelatedPlaces(t_2) = \{p_1, p_2, p_3, p_6, p_7, p_8\}$  and  $UnrelatedPlaces(t_1) = UnrelatedPlaces(t_2) = \{p_4, p_5\}$ . If  $\Psi(p_3; p_7; p_4) > \eta_1$  and  $\Upsilon(p_1, p_2; p_6; p_5) > \eta_2$ ,  $p_4$  has a catalytic effect on  $t_2$  and  $p_5$  has an inhibitory effect on  $t_1$ . As shown in SBTPN  $G_3$  in Fig. S3, a green dashed arc from  $p_4$  to  $t_2$  and a red dotted arc from  $p_5$  to  $t_1$  are defined to represent the above catalytic and inhibitory effects, respectively. Their corresponding time delays, which can be calculated by Definition 2, are expressed as  $E(p_4, p_7) = e_{47}$  and  $E(p_5, p_6) = e_{56}$ , respectively.

The procedure for mining the synergy effects constrained by time is summarized in Algorithm 3.

---

**Algorithm 3** Mining synergy effects constrained by time

**Input:** MTS  $X$  with dataset  $\partial$ ; PN  $G_2$  learned by Algorithm 2; thresholds  $\eta_1$  and  $\eta_2$  used to determine synergy effects.

**Output:** An SBTPN  $G_3$ .

```

1: for  $\forall t_k \in G_2$  do
2:   for  $\forall p_x \in UnrelatedPlaces(t_k)$  do
3:     if  $\Psi(\cdot; t_k; t_k'; p_x) > \eta_1$  then
4:       Define a green dashed arc from  $p_x$  to  $t_k$ ;
5:     end if
6:     if  $\Upsilon(\cdot; t_k; t_k'; p_x) > \eta_2$  then
7:       Define a red dotted arc from  $p_x$  to  $t_k$ ;
8:     end if

```

9: Denote by  $p_j$  the output place of  $t_k$  ;  
10: Let  $E(p_x, p_j) = e_{xj}$  , where  $e_{xj}$  is calculated by  
Definition 2;  
11: **end for**  
12: **end for**  
13: **return** an SBTPN  $G_3$

Noise can interfere with the discovery of causal relations, especially “AND” relations and synergy effects. Specifically, for the “AND” and “OR” structures pointing to the same effect variable, identifying the “AND” structures becomes more difficult as the number of the “OR” structures increases. This is because the “OR” structure can weaken the influence of the cause variables within the “AND” structure on the effect variable, making it difficult to discover the causal relations among these variables and thus identify the entire “AND” structure. Moreover, noise is a prerequisite for the existence of synergy effects. If a causal effect is deterministic (i.e., always occurs), synergy effect will not exist. The amount of synergy information carried by synergy variables increases as the noise ratio increases in a certain range, thus making the synergy effects easier to identify.

#### IV. SBTPN-BASED RCA

This section proposes an RCA method considering “AND/OR” relations and synergy effects based on SBTPN.

For a place  $p_j$  in an SBTPN, let  $CauseSet(p_j)$  denote the places corresponding to the direct or indirect causes of variable  $\beta(p_j)$ , and  $\hat{p}_j$  represent that  $\beta(p_j)$  is in an abnormal state. Consider SBTPN  $G_3$  in Fig. S3. We have  $CauseSet(p_8) = \{p_1, p_2, p_3, p_6, p_7\}$ . Any variable  $\beta(p_i)$  satisfying  $p_i \in CauseSet(p_j)$  may be the root cause of the abnormality of  $\beta(p_j)$ .  $\Pr(\hat{p}_i|\hat{p}_j)$  depicts the possibility that  $\hat{p}_i$  is the root cause of  $\hat{p}_j$ . For a transition  $t_k \in p_i^*$  located in the causal path from  $\beta(p_i)$  to  $\beta(p_j)$ , if it is affected by synergy effects, the value of  $\Pr(\hat{p}_i|\hat{p}_j)$  is changed. Let  $\Pr(\hat{p}_i|\hat{p}_j)$  denote the probability that  $\hat{p}_i$  is the root cause of  $\hat{p}_j$  considering all synergy effects imposed on  $t_k$ , which can be characterized by (8) in the paper.

Let  $\delta = \max\{\Pr(\hat{p}_i|\hat{p}_j) | p_i \in CauseSet(p_j)\}$  such that  $\delta \geq 0.5$ . It is a benchmark used to identify the potential root causes of  $\beta(p_j)$  from  $CauseSet(p_j)$ . For  $\forall p_i \in CauseSet(p_j)$ , if  $\Pr(\hat{p}_i|\hat{p}_j) \in [0.5, \delta]$ ,  $p_i$  is added to a set denoted by  $Candidate(p_j)$ . It records the potential root causes of  $\beta(p_j)$ . Let  $TranSet(p_a, p_b)$  denote the set of transitions located in the causal path from variable  $\beta(p_a)$  to variable  $\beta(p_b)$ . For  $\forall p_q \in Candidate(p_j)$ , if  $\exists t_u \in p_q^* \cap TranSet(p_q, p_j)$  such that  $p_s \in t_u \wedge p_s \notin Candidate(p_j)$ ,  $p_q$  is removed from  $Candidate(p_j)$ . Let  $I(p)$  denote the set of input places of  $p$ . Consider SBTPN  $G_3$  in Fig. S3. We have  $I(p_8) = \{p_6, p_7\}$ . For  $\forall p_1, p_2, \dots, p_u \in Candidate(p_j)$  such that  $p_1 \in I(p_j)$  and

$p_k \in I(p_{k-1})$  ( $k = 2, 3, \dots, u$ ), if  $p_g \notin Candidate(p_j)$  for  $\forall p_g \in I(p_u)$ ,  $p_u$  is added to a set denoted by  $RootCause(p_j)$ . The variables corresponding to the places in  $RootCause(p_j)$  are the root causes of  $\beta(p_j)$ .

*Example 3:* Consider SBTPN  $G_3$  in Fig. S3. Suppose  $\delta = \Pr(\hat{p}_6|\hat{p}_8) \geq 0.5$ . If  $\Pr(\hat{p}_2|\hat{p}_8), \Pr(\hat{p}_3|\hat{p}_8), \Pr(\hat{p}_6|\hat{p}_8), \Pr(\hat{p}_7|\hat{p}_8) \in [0.5, \delta]$ , we have  $Candidate(p_8) = \{p_3, p_6, p_7\}$ . Since  $p_6 \in I(p_8)$ ,  $p_6 \in Candidate(p_8)$ ,  $p_1, p_2 \in I(p_6)$ , and  $p_1, p_2 \notin Candidate(p_8)$ ,  $p_6$  is added to  $RootCause(p_8)$ . Since  $p_7 \in I(p_8)$ ,  $p_7 \in Candidate(p_8)$ ,  $p_3 \in I(p_7)$ ,  $p_3 \in Candidate(p_8)$ , and  $I(p_3) = \emptyset$ ,  $p_3$  is added to  $RootCause(p_8)$ . Thus, the root causes of  $\beta(p_8)$  are  $\beta(p_3)$  and  $\beta(p_6)$ .

The process for discovering the root causes of abnormal events is realized via Algorithm 4.

#### Algorithm 4 RCA for abnormal events

**Input:** MTS  $X$  with dataset  $\partial$  ; SBTPN  $G_3$  learned by Algorithm 3; place set  $P_A$  corresponding to abnormal events.

**Output:** Root causes of abnormal events.

```

1: for  $\forall p_j \in P_A$  do
2:   for  $\forall p_i \in CauseSet(p_j)$  do
3:     Calculate  $\Pr(\hat{p}_i|\hat{p}_j)$  using (6)-(8);
4:   end for
5:   Let  $\delta = \max\{\Pr(\hat{p}_i|\hat{p}_j) | p_i \in CauseSet(p_j)\}$ ;
6:   if  $\delta < 0.5$  then
7:     continue;
8:   end if
9:   for  $\forall p_i \in CauseSet(p_j)$  do
10:    if  $\Pr(\hat{p}_i|\hat{p}_j) \in [0.5, \delta]$  then
11:      Add  $p_i$  to  $Candidate(p_j)$ ;
12:    end if
13:  end for
14:  for  $\forall p_q \in Candidate(p_j)$  do
15:    if  $\exists t_u \in p_q^* \cap TranSet(p_q, p_j)$  such that  $p_s \in t_u \wedge p_s \notin Candidate(p_j)$  then
16:      Remove  $p_q$  from  $Candidate(p_j)$ ;
17:    end if
18:  end for
19:  for  $\forall p_1, p_2, \dots, p_u \in Candidate(p_j)$  such that  $p_1 \in I(p_j) \wedge p_k \in I(p_{k-1})$  ( $k = 2, 3, \dots, u$ ) do
20:    if  $p_g \notin Candidate(p_j)$  for  $\forall p_g \in I(p_u)$  then
21:      Add  $p_u$  to  $RootCause(p_j)$ ;
22:    end if
23:  end for
24: end for
25: return the root causes of  $P_A$ 

```

## EXPERIMENTAL DETAILS

### A. Parameter Sensitivity Analysis

This section utilizes the solar panel manufacturing case presented in Section VII of the paper to discuss the sensitivity of SBTPN to parameter settings. SBTPN is sensitive to threshold values  $\eta_1$  for determining catalytic effects and  $\eta_2$  for determining inhibitory effects, where  $\eta_1, \eta_2 \in [0.5, 1)$ . From Fig. S4, SBTPN loses its ability to identify synergy effects when the values of  $\eta_1$  or  $\eta_2$  are high. This is because a stronger catalytic (inhibitory) effect results in a stronger correlation between the corresponding catalytic (inhibitory) factor and the effect variable, thereby increasing the likelihood of misinterpreting the catalytic (inhibitory) effect as a causal one. Moreover, a low value of  $\eta_2$  negatively impacts the performance of SBTPN in identifying synergy effects. This is because noise can interfere with the identification of synergy effects, and a low synergy identification threshold is unable to eliminate this interference. From the above analysis, the thresholds for identifying synergy effects should be determined cautiously.

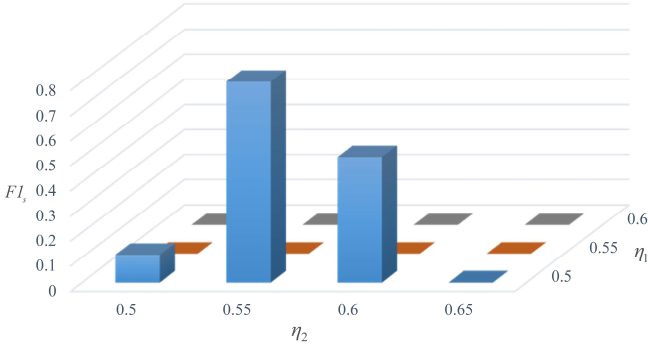


Fig. S4. Performance of SBTPN in identifying synergy effects under different combinations of  $\eta_1$  and  $\eta_2$ .

### B. Principles of RCA

This section defines the principles of RCA based on the compared methods discussed in Section VII-A of the paper.

For an anomalous variable  $x_j^r$  in Fig. S5, if its direct/indirect cause  $x_i^{r-k}$  is also in an abnormal state such that  $k$  is consistent with the time delay of  $x_i$  affecting  $x_j$  given in Fig. S5,  $x_i^{r-k}$  is added to a set denoted by  $PotenRoot(x_j^r)$ .

$PotenRoot(x_j^r)$  denotes the potential root causes of  $x_j^r$ . Consider the case that the products  $x_{20}^r$ ,  $x_{17}^{r-1}$ ,  $x_{14}^{r-3}$ , and  $x_{10}^{r-6}$  in Fig. S5 are all unqualified. By the temporal causal relations in Fig. S5, we have  $PotenRoot(x_{20}^r) = \{x_{17}^{r-1}, x_{14}^{r-3}\}$ . Let  $AntTran(x_j)$  denote the set of the transitions that directly/indirectly point to variable  $x_j$ ,  $DireCause(t)$  denote the set of  $t$ 's input places-associated variables, and  $Cause(t)$  denote the set of the variables in  $DireCause(t)$  and their direct/indirect causes. Consider the variable  $x_{14}$  and the transition  $t_{11}$  in Fig. S5. We have  $AntTran(x_{14}) = \{t_1, t_2, t_5, t_6\}$ ,

$DireCause(t_{11}) = \{x_{14}\}$ , and  $Cause(t_{11}) = \{x_1, x_2, x_3, x_4, x_{10}, x_{11}, x_{14}\}$ . The following four rules are adopted to determine the true root causes of  $x_j^r$ .

**Rule 1:** For a transition  $t \in AntTran(x_j)$  such that  $t$  is affected by inhibitory effects, the abnormality of  $x_i \in Cause(t)$  is not the cause of the abnormality of  $x_j$ .

Therefore,  $x_i$  is removed from  $PotenRoot(x_j^r)$ .

**Rule 2:** For a transition  $t \in AntTran(x_j)$ , if  $\exists x_a, x_b \in DireCause(t)$  such that at least one of them is in a normal state, the abnormality of  $x_i \in Cause(t)$  is not the cause of the abnormality of  $x_j$ . Thus  $x_i$  is removed from  $PotenRoot(x_j^r)$ .

**Rule 3:** For a transition  $t \in AntTran(x_j)$ , if  $\exists x_i \in Cause(t)$  such that it is in a normal state, the abnormality of the direct/indirect cause  $x_h$  of  $x_i$  is not the cause of the abnormality of  $x_j$ . Therefore,  $x_h$  is removed from  $PotenRoot(x_j^r)$ .

**Rule 4:** By the above three rules,  $PotenRoot(x_j^r)$  is updated. For the updated  $PotenRoot(x_j^r)$ , if  $\exists x_i \in PotenRoot(x_j^r)$  such that  $x_k$  is not the cause of  $x_i$  for  $\forall x_k \in PotenRoot(x_j^r) \setminus x_i$ ,  $x_i$  is the root cause of  $x_j^r$ .

The temporal causal structure in Fig. S5 is used to illustrate the above rules. Consider the following cases.

**Case 1:**  $x_{20}^r$ ,  $x_{17}^{r-1}$ ,  $x_{14}^{r-3}$ , and  $x_{10}^{r-5}$  are all unqualified, and  $x_{29}^{r-2}$  is true (i.e.,  $x_{14}^{r-3}$  is quality checked at time  $\tau-2$ ). We have  $PotenRoot(x_{20}^r) = \{x_{10}^{r-5}, x_{14}^{r-3}, x_{17}^{r-1}\}$ . By Rule 1, we can get that the abnormality of  $x_{10}^{r-5}$  or  $x_{14}^{r-3}$  is not the cause of the abnormality of  $x_{20}^r$ . According to Rule 4, the cause of  $x_{20}^r$  being unqualified is  $x_{17}^{r-1}$  being unqualified.

**Case 2:**  $x_{14}^r$ ,  $x_{10}^{r-2}$ , and  $x_1^{r-3}$  are all unqualified, but  $x_2^{r-3}$  is qualified. We have  $PotenRoot(x_{14}^r) = \{x_1^{r-3}, x_{10}^{r-2}\}$ . According to Rule 2, the abnormality of  $x_1^{r-3}$  is not the cause of the abnormality of  $x_{14}^r$ . By Rule 4, the cause of  $x_{14}^r$  being unqualified is  $x_{10}^{r-2}$  being unqualified.

**Case 3:**  $x_{20}^r$ ,  $x_{17}^{r-1}$ , and  $x_{10}^{r-5}$  are all unqualified, but  $x_{14}^{r-3}$  is qualified. We have  $PotenRoot(x_{20}^r) = \{x_{10}^{r-5}, x_{17}^{r-1}\}$ . By Rule 3, the abnormality of  $x_{10}^{r-5}$  is not the cause of the abnormality of  $x_{20}^r$ . According to Rule 4, the cause of  $x_{20}^r$  being unqualified is  $x_{17}^{r-1}$  being unqualified.

The Syn500 dataset discussed in the paper is used to evaluate the performance of the compared methods in RCA. This study focuses on the abnormalities of end products  $x_{20}$ ,  $x_{21}$ , and  $x_{22}$  in Fig. S5. According to the causal relations in Fig. S6(a) and Rules 1-4, the true root causes of abnormalities

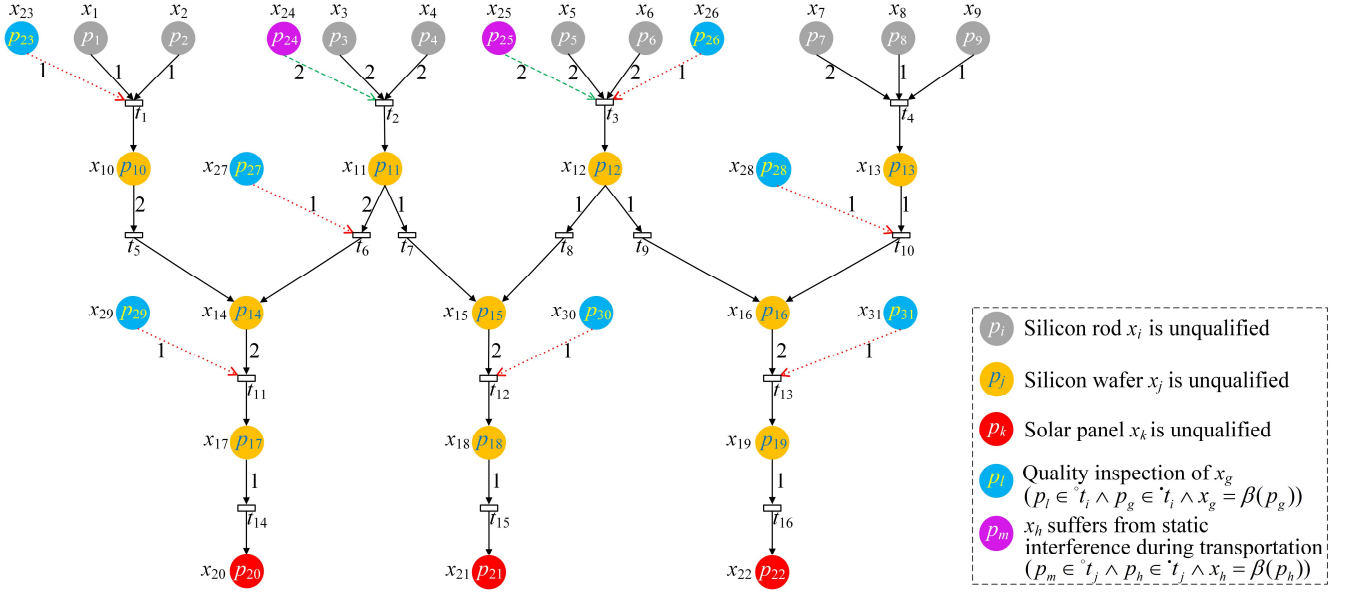


Fig. S5. Quality anomalies of solar panel manufacturing process.

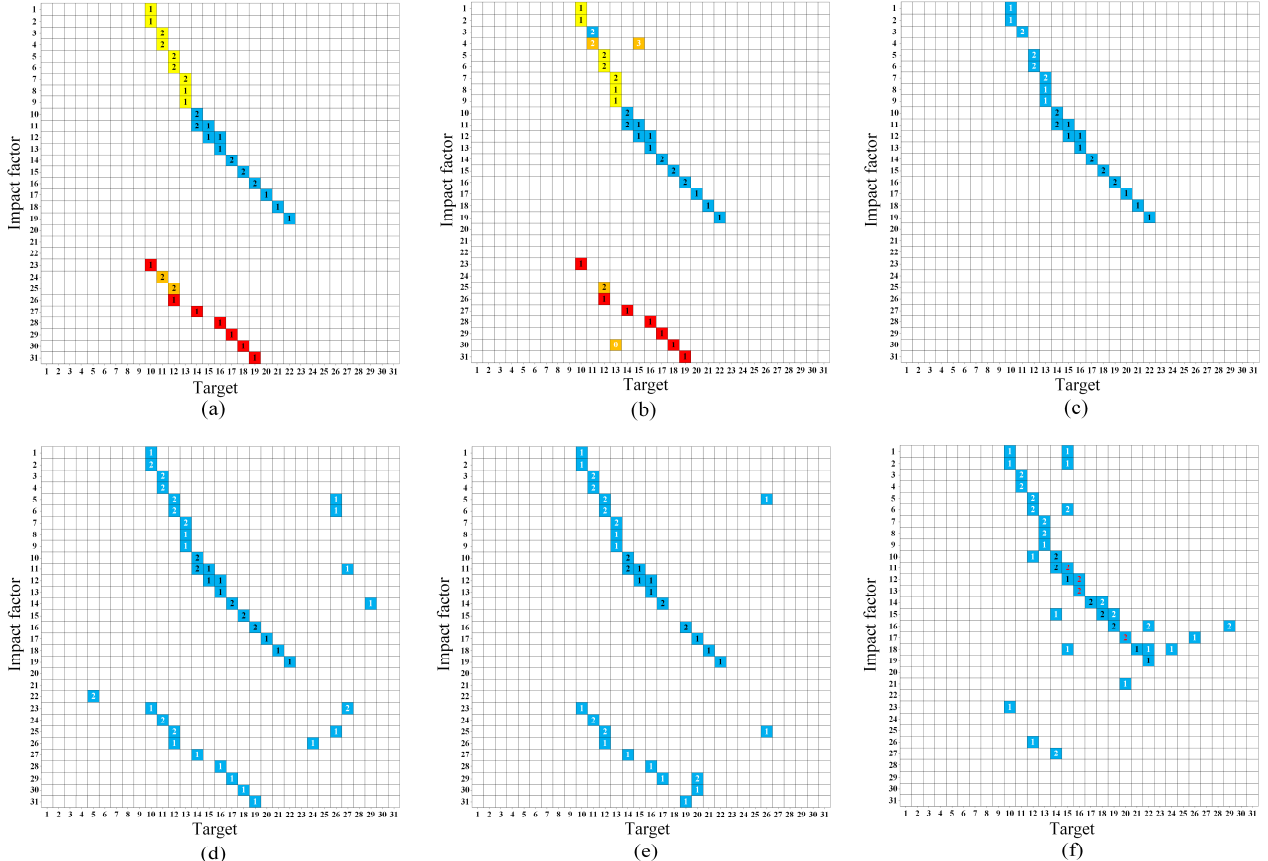


Fig. S6. Causality matrices generated by all compared methods. (a) Ground truth, (b) SBTPN, (c) TCDF, (d) MTE, (e) PCMCI, and (f) MLP-GC.

of  $x_{20}$ ,  $x_{21}$  and  $x_{22}$  on Syn500 can be identified. Since all the competing methods fail to consider “AND” relations as well as synergy effects, the root causes of these three variables predicted by them on Syn500 can be obtained by using the causal relations in Figs. S6(c)-(f) as well as Rules 3 and 4. The root causes of these variables predicted by the proposed

SBTPN on Syn500 can be derived by using the causal relations in Fig. S6(b) and Algorithm 4.

#### REFERENCE

- [1] M. Nauta, D. Bucur, and C. Seifert, “Causal discovery with attention-based convolutional neural networks,” *Mach. Learn. Knowl. Extr.*, vol.1, no.1, pp.312–340, 2019.